Journal of Statistical and Econometric Methods, vol. 2, no.3, 2013, 17-40
ISSN: 2051-5057 (print version), 2051-5065(online)
Scienpress Ltd, 2013

An *L*-Moment Based Characterization of the Family of Dagum Distributions

Mohan D. Pant[1] and Todd C. Headrick[2]

Abstract

This paper introduces a method for simulating univariate and multivariate Dagum distributions through the method of *L*-moments and *L*-correlations. A method is developed for characterizing non-normal Dagum distributions with controlled degrees of *L*-skew, *L*-kurtosis, and *L*-correlations. The procedure can be applied in a variety of contexts such as statistical modeling (e.g., income distribution, personal wealth distributions, etc.) and Monte Carlo or simulation studies. Numerical examples are provided to demonstrate that *L*-moment-based Dagum distributions are superior to their conventional moment-based analogs in terms of estimation and distribution fitting. Evaluation of the proposed method also demonstrates that the estimates of *L*-skew, *L*-kurtosis, and *L*-correlation are substantially superior to their conventional product-moment based counterparts of skew, kurtosis, and Pearson correlation in terms of relative bias and relative efficiency–most notably in the context of heavy-tailed distributions.

Mathematics Subject Classification: 60E05, 62G30, 62H12, 62H20, 65C05, 65C10, 65C60, 78M05
Keywords: Skew, *L*-skew, Kurtosis, *L*-kurtosis, Correlation, *L*-correlation.

1 Introduction

The family of Dagum distributions is commonly used for fitting income and personal wealth data. For example, some of the countries for which personal income data were fitted by Dagum distributions are Argentina, Canada, Sri Lanka, and the USA [2]. For a list of other applications of Dagum distributions, see [13].The cumulative distribution function (cdf) associated with Dagum distributions is given as [1, 13]:

[1]University of Texas at Arlington, Arlington, TX 76019, USA.
[2]Southern Illinois University Carbondale, Carbondale, IL 62901, USA.

Article Info: *Received :* June 14, 2013. *Revised :* July 6, 2013.
Published online : September 9, 2013

$$F(x) = \left(1 + \left(\frac{x}{b}\right)^{-a}\right)^{-p} \tag{1}$$

where $x \in (0, \infty), p, a, b > 0$ and where p and a are shape parameters and b is a scale parameter, respectively. These parameters determine the mean, variance, skew, and kurtosis of a distribution. The quantile function associated with the cdf in (1) is given as in [13]

$$F^{-1}(x) = q(u) = b\left(u^{-1/p} - 1\right)^{-1/a} \tag{2}$$

where $u \sim iid\ U(0, 1)$. The scale and shape of a Dagum distribution associated with (2) are dependent on the values of the parameters b, p, and a, which can be determined by simultaneously solving (A.7)—(A.9) in the Appendix for the given values of standard deviation (σ), skew (γ_3), and kurtosis (γ_4). In order for the equation (2) to produce a valid Dagum pdf, the quantile function $q(u)$ is required to be a strictly increasing monotone function [8]. This requirement implies that an inverse function (q^{-1}) exists. As such, the cdf associated with (2) can be expressed as $F\big(q(u)\big) = F(u) = u$ and subsequently differentiating this cdf with respect to u will yield the parametric form of the pdf for $q(u)$ as $f\big(q(u)\big) = 1/q'(u)$. We would also note that the simple closed-form expression for the pdf associated with (1) can be given as [13]

$$f(x) = apb^a x^{-(a+1)} \left(1 + \left(\frac{x}{b}\right)^{-a}\right)^{-(p+1)} \tag{3}$$

Some of the problems associated with conventional moment-based estimates are that they can be (a) substantially biased, (b) highly dispersed, or (c) influenced by outliers [3, 9], and thus may not be good representatives of the true parameters. To demonstrate, Figure 1 gives the graphs of the pdf and cdf associated with the Dagum distribution with shape and scale parameters as $p = 0.36$, $a = 4.273$, and $b = 14.28$. These values of shape and scale parameters are associated with the Dagum distribution fitted to the 1969 US family income data given in Dagum (1980, p. 360) as cited in [13, p. 107]. These values of p, a, and b were substituted into (A.6)—(A.9) to determine the values for the mean (μ), standard deviation (σ), skew (γ_3), and kurtosis (γ_4) associated with the pdf in Figure 1. Table 1 gives the parameters and sample estimates for the mean, standard deviation, skew, and kurtosis for the distribution in Figure 1. Inspection of Table 1 indicates that the bootstrap estimates (S, g_3, and g_4) of standard deviation, skew, and kurtosis (σ, γ_3, and γ_4) are substantially attenuated below their corresponding parameter values with greater bias and variance as the order of the estimate increases. Specifically, for sample size of n = 50, the values of the estimates are only 96.06%, 47.26%, and 4.14% of their corresponding parameters, respectively. The estimates (S, g_3, and g_4) of standard deviation, skew, and kurtosis (σ, γ_3, and γ_4) in Table 1 were calculated based on Fisher's k-statistics formulae [16, pp. 299-300], which are currently used by most commercial software packages such as SAS, SPSS, Minitab, etc., for computing the values of skew and kurtosis (where $\sigma = 1$ and $\gamma_{3,4} = 0$ for the standard normal distribution).

Another unfavorable quality associated with conventional moment-based estimators of skew and kurtosis is that their values are algebraically bounded by the sample size (n)

such that $|g_3| \leq \sqrt{n}$ and $g_4 \leq n$ [3]. This constraint implies that if a researcher wants to simulate non-normal data with kurtosis $\gamma_4 = 66.3722$ as in Table 1 by drawing a sample of size $n = 50$ from this population, then the largest possible value of the computed estimate (g_4) of kurtosis (γ_4) is only 50, which is only 75.33% of the parameter.

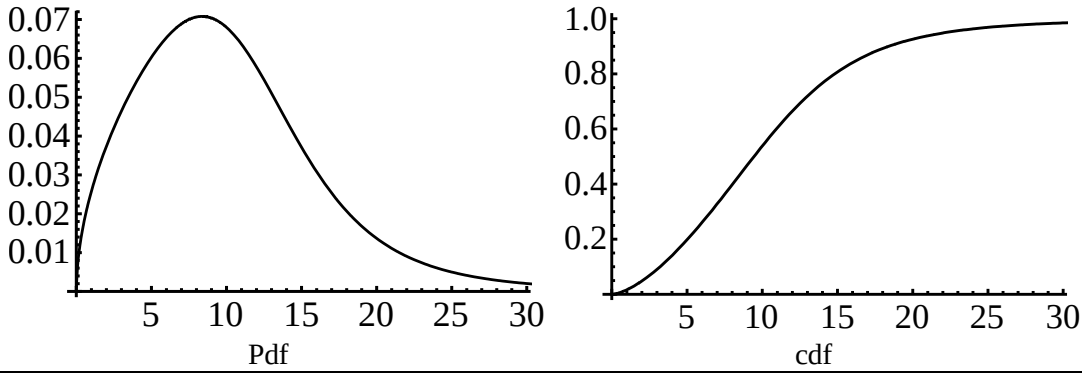

Figure 1: The pdf and cdf of a Dagum distribution with shape and scale parameters of $p = 0.36$, $a = 4.273$, and $b = 14.28$. The parameter values of mean (μ), standard deviation (σ), skew (γ_3), and kurtosis (γ_4) associated with this distribution are given in Table 1.

Table 1: Conventional moment-based parameters $(\mu, \sigma, \gamma_3, \gamma_4)$ of mean, standard deviation, skew, and kurtosis and their estimates (M, S, g_3, g_4) for the pdf in Figure 1. Each bootstrapped estimate (Estimate), associated 95% bootstrap confidence interval (95% Bootstrap C.I.), and the standard error (St. Error) were based on resampling 25,000 statistics. Each statistic was based on a sample size of $n = 50$.

Parameter	Estimate	95% Bootstrap C.I.	St. Error
$\mu = 10.4572$	$M = 10.46$	$(10.451, 10.474)$	0.00603
$\sigma = 6.8354$	$S = 6.566$	$(6.5479, 6.5874)$	0.01004
$\gamma_3 = 2.5838$	$g_3 = 1.221$	$(1.2103, 1.2313)$	0.00539
$\gamma_4 = 66.3722$	$g_4 = 2.751$	$(2.6937, 2.8126)$	0.03052

The method of L-moments introduced by Hosking [9] is an attractive alternative to conventional moments and can be used for describing theoretical probability distributions, fitting distributions to real-world data, estimating parameters, and hypothesis testing [3, 9, 11]. In these contexts, we note that the L-moment based estimators of L-skew, L-kurtosis, and L-correlation have been introduced to address the limitations associated with conventional moment-based estimators [3, 4-7, 9-12, 15, 19]. Some qualities of L-moments that make them superior to conventional moments are that they (a) exist for any distribution with finite mean, (b) have estimates that are nearly unbiased for any sample size and less affected from sampling variability, (c) are more robust in the presence of outliers in the sample data, and (d) are not algebraically bounded by sample size [3, 9-11]. For example, the estimates of L-scale, L-skew, and L-kurtosis (ℓ_2, t_3, and t_4) in Table 2 are relatively closer to their respective parameter values $(\lambda_2, \tau_3$, and $\tau_4)$ and have smaller variance relative to their conventional moment-based counterparts as in

Table 1. Inspection of Table 2 indicates that for the sample size of $n = 50$, the values of the estimates are on average 99.95%, 95.09% and 96.73% of their corresponding parameters.

Table 2: L-moment based parameters $(\lambda_1, \lambda_2, \tau_3, \tau_4)$ of L-mean, L-scale, L-skew, and L-kurtosis and their estimates $(\ell_1, \ell_2, t_3, t_4)$ for the pdf in Figure 1. Each bootstrapped estimate (Estimate), associated 95% bootstrap confidence interval (95% Bootstrap C.I.), and the standard error (St. Error) were based on resampling 25,000 statistics. Each statistic was based on a sample size of $n = 50$.

Parameter	Estimate	95% Bootstrap C.I.	St. Error
$\lambda_1 = 10.4572$	$\ell_1 = 10.46$	$(10.451, 10.474)$	0.00603
$\lambda_2 = 3.5057$	$\ell_2 = 3.504$	$(3.4971, 3.5108)$	0.00348
$\tau_3 = 0.1914$	$t_3 = 0.182$	$(0.1810, 0.1831)$	0.00054
$\tau_4 = 0.1683$	$t_4 = 0.1628$	$(0.1619, 0.1637)$	0.00046

In view of the above, the primary purpose of this study is to characterize the family of Dagum distributions through the method of L-moments to obviate the problems associated with conventional moment-based estimators. Further, another aim of this study is to develop the methodology for simulating Dagum distributions with specified L-correlation matrices [19]. Specifically, in Section 2, a brief introduction to univariate L-moments is provided. The systems of equations associated with the Dagum distributions are subsequently derived for determining the shape and scale parameters (p, a, and b) for user specified values of L-scale (λ_2), L-skew (τ_3), and L-kurtosis (τ_4). In Section 3, a comparison between conventional and L-moment-based Dagum distributions is presented in the contexts of estimation and distribution fitting. Numerical examples based on Monte Carlo simulation techniques are also provided to confirm the methodology and demonstrate the advantages that L-moments have over conventional moments. In Section 4, an introduction to the coefficient of L-correlation is provided as well as the methodology for simulating Dagum distributions with specified L-correlations. In Section 5, the steps for implementing the proposed L-moment procedure are described for simulating non-normal Dagum distributions with controlled values of standard deviation (L-scale), skew (L-skew), kurtosis (L-kurtosis), and Pearson correlations (L-correlations). Numerical examples and the results of a simulation are also provided to confirm the derivations and compare the new procedure with the conventional moment-based procedure. In Section 6, the results of the simulation are discussed.

2 Methodology

2.1 Theoretical and Empirical Definitions of L-Moments

L-moments can be expressed as certain linear combinations of probability weighted moments (PWMs). Specifically, let $X_1, \dots, X_i, \dots, X_n$ be identically and independently distributed random variables each with pdf $f(x)$, cdf $F(x)$, and the quantile function $F^{-1}(x)$. As such, the PWMs are defined as [3, equation (2.1)]

$$\beta_r = \int F^{-1}(x)\{F(x)\}^r f(x)dx \tag{4}$$

where $r = 0, 1, 2, 3$. The first four L-moments $(\lambda_{i=1,\dots,4})$ associated with X can be expressed in simplified forms as [11, pp. 20-22]

$$\lambda_1 = \beta_0 \tag{5}$$
$$\lambda_2 = 2\beta_1 - \beta_{0,} \tag{6}$$
$$\lambda_3 = 6\beta_2 - 6\beta_1 + \beta_0, \tag{7}$$
$$\lambda_4 = 20\beta_3 - 30\beta_2 + 12\beta_1 - \beta_{0,} \tag{8}$$

where the coefficients associated with $\beta_{r=0,\dots,3}$ in (5)—(8) are obtained from shifted orthogonal Legendre polynomials and are computed as in [11, pp. 20-22] or in [3, pp. 4-5].

The notations λ_1 and λ_2 denote the location and scale parameters. Specifically, in the literature of L-moments, λ_1 is referred to as the L-location parameter, which is equal to the arithmetic mean, and λ_2 (> 0) is referred to as the L-scale parameter and is one-half of Gini's coefficient of mean difference [16, pp. 47-48]. Dimensionless L-moment ratios are defined as the ratios of higher-order L-moments (i.e., λ_3 and λ_4) to λ_2. Thus, $\tau_3 = \lambda_3/\lambda_2$ and $\tau_4 = \lambda_4/\lambda_2$ are, respectively, the indices of L-skew and L-kurtosis. In general, the indices of L-skew and L-kurtosis are bounded in the interval $-1 < \tau_{3,4} < 1$, and as in conventional moment theory, a symmetric distribution has L-skew equal to zero [3]. The boundary region for L-skew (τ_3) and L-kurtosis (τ_4) for a continuous distribution is given by the inequality [14]

$$\frac{5\tau_3^2 - 1}{4} < \tau_4 < 1 \tag{9}$$

Empirical L-moments for a sample (of size n) of real-world data are expressed as linear combinations of the unbiased estimators of the PWMs based on sample order statistics $X_{1:n} \le X_{2:n} \le \cdots \le X_{n:n}$. Specifically, the unbiased estimators of the PWMs are given as [9, pp. 113-114]

$$b_r = \frac{1}{n}\sum_{i=r+1}^{n} \frac{(i-1)(i-2)\dots(i-r)}{(n-1)(n-2)\dots(n-r)} X_{i:n} \tag{10}$$

where $r = 0, 1, 2, 3$ and b_0 is the sample mean. The first four sample L-moments $(\ell_1, \ell_2, \ell_3, \ell_4)$ are obtained by substituting b_r from (10) instead of β_r in equations (5)−(8). The sample L-moment ratios (i.e., L-skew and L-kurtosis) are denoted as t_3 and t_4, where $t_3 = \ell_3/\ell_2$ and $t_4 = \ell_4/\ell_2$.

2.2 *L*-Moment Based System for Dagum Distributions

If we substitute $F^{-1}(x) = b\left(u^{-1/p} - 1\right)^{-1/a}$ from (2), where $F(x) = u$ and $f(x) = 1$ in (4), then the r-th PWM for the family of Dagum distributions is given as

$$\beta_r = \int_0^1 b\left(u^{-1/p} - 1\right)^{-1/a} u^r \, du. \tag{11}$$

Equation (11) can also be expressed as:

$$\beta_r = bp \int_0^1 \left(u^{1/p}\right)^{(p+pr+1/a)-1} \left(1 - u^{1/p}\right)^{-1/a} \left(p^{-1} u^{(1/p)-1} du\right). \tag{12}$$

Let $u^{1/p} = x$. As such, we have $p^{-1}u^{(1/p)-1}du = dx$ and subsequently substituting this result into (12) yields the r-th PWM, which can be expressed as

$$\beta_r = bp \int_0^1 x^{(p+pr+1/a)-1} (1-x)^{(1-1/a)-1} \, dx. \tag{13}$$

Integrating (13) for $\beta_{r=0,1,2,3}$ and substituting these PWMs into (5)—(8) and simplifying gives the following L-moment based system of equations for the family of Dagum distributions as

$$\lambda_1 = (b\Gamma[1 - 1/a]\Gamma[p + 1/a])/\Gamma[p] \tag{14}$$

$$\lambda_2 = b\Gamma[1 - 1/a]\,(\Gamma[p]\Gamma[2p + 1/a] - \Gamma[2p]\Gamma[p + 1/a])/(\Gamma[p]\Gamma[2p]) \tag{15}$$

$$\begin{aligned} \tau_3 = \{&\Gamma[1 + 3p](6\Gamma[1 + p]\Gamma[2p + 1/a] - \Gamma[1 + 2p]\Gamma[p + 1/a]) - \\ &6\Gamma[1 + p]\Gamma[1 + 2p]\Gamma[3p + 1/a]\}/ \\ &\{\Gamma[1 + 3p](\Gamma[1 + 2p]\Gamma[p + 1/a] - 2\Gamma[1 + p]\Gamma[2p + 1/a])\} \end{aligned} \tag{16}$$

$$\begin{aligned} \tau_4 = \{&\Gamma[1 + 4p]\{\Gamma[1 + 3p](\Gamma[1 + 2p]\Gamma[p + 1/a] - 12\Gamma[1 + p] \times \\ &\Gamma[2p + 1/a]) + 30\Gamma[1 + p]\Gamma[1 + 2p]\Gamma[3p + 1/a]\} - \\ &20\Gamma[1 + p]\Gamma[1 + 2p]\Gamma[1 + 3p]\,\Gamma[4p + 1/a]\}/\{\Gamma[1 + 3p] \times \\ &\Gamma[1 + 4p](\Gamma[1 + 2p]\Gamma[p + 1/a] - 2\Gamma[1 + p]\Gamma[2p + 1/a])\} \end{aligned} \tag{17}$$

Note that equations (16) and (17) have been derived in a similar context for Burr Type III distributions by Pant and Headrick [15]. Given specified values of L-scale (λ_2), L-skew (τ_3), and L-kurtosis (τ_4) the systems of equations (15)−(17) can be simultaneously solved for real values of p, a, and b. The solved values of p, a, and b can be substituted into (2) for generating Dagum distributions. Further, the solved values of p, a, and b can be substituted in (14) for computing the value of L-mean (λ_1). In the next section, two examples are provided to demonstrate the aforementioned methodology and the advantages that L-moments have over conventional moments in the contexts of estimation and distribution fitting.

3 Comparison of L-Moments with Conventional Moments

3.1 Estimation

To demonstrate the advantages of L-moment-based estimation over conventional moment-based estimation, an example is provided in Tables 6 and 7 in the context of four Dagum distributions depicted in Figure 2. Specifically, Figure 2 gives the pdfs of four asymmetric Dagum distributions with their corresponding conventional-moment-based parameters of skew (γ_3) and kurtosis (γ_4), L-moment-based parameters of L-scale (λ_2), L-skew (τ_3), and L-kurtosis (τ_4), and their respective shape and scale parameters of p, a, and b. The values of p, a, and b are determined by simultaneously solving equations (A.7)—(A.9) from the Appendix using the standard deviation $\left(\sigma = 1/\sqrt{12}\right)$ associated with the uniform distribution and the specified values of skew (γ_3) and kurtosis (γ_4). The solutions of p, a, and b are used in (15)—(17) to determine the L-moment based parameters of L-scale (λ_2), L-skew (τ_3), and L-kurtosis (τ_4) as well as in equation (3) to produce the pdfs that are given in Figure 2.

The advantages of L-moment-based estimators have over those based on conventional moments can also be demonstrated in the context of Dagum distributions by considering the Monte Carlo simulation results associated with the indices for the percentage of relative bias (RB%) and standard error (St. Error) reported in Tables 6 and 7.

Specifically, a Fortran [18] algorithm was written to simulate 25,000 independent samples of sizes $n = 25, 1000$ and the conventional-moment based estimates (g_3 and g_4) of skew and kurtosis (γ_3 and γ_4) and the L-moment based estimates (t_3 and t_4) of L-skew and L-kurtosis (τ_3 and τ_4) were computed for each of the $(2 \times 25{,}000)$ samples based on the parameters and the values of p, a, and b listed in Figure 2. The estimates (g_3 and g_4) of γ_3 and γ_4 were computed based on Fisher's k-statistics [16, pp. 47-48], whereas the estimates (t_3 and t_4) of τ_3 and τ_4 were computed using (16) and (17). Bias-corrected accelerated bootstrapped average estimates (Estimate), associated 95% confidence intervals (95% Bootstrap C.I.), and standard errors (St. Error) were obtained for each type of estimates using 10,000 resamples via the commercial software package Spotfire S+ [20]. Further, if a parameter was outside its associated 95% bootstrap C.I., then the percentage of relative bias (RB%) was computed for the estimate as:

$$\text{RB\%} = 100 \times (\text{Estimate} - \text{Parameter})/\text{Parameter} \tag{18}$$

1	$\gamma_3 = -0.5$ $\gamma_4 = 1.5$ $\lambda_2 = 0.1579718$ $\tau_3 = -0.075116$ $\tau_4 = 0.172709$ $p = 0.520053$ $a = 42.352031$ $b = 5.136684$	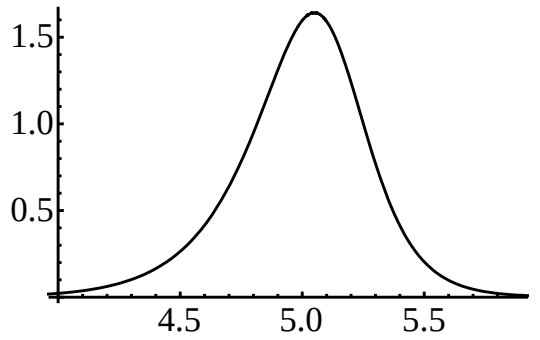
2	$\gamma_3 = -1$ $\gamma_4 = 2.5$ $\lambda_2 = 0.155298$ $\tau_3 = -0.142370$ $\tau_4 = 0.178771$ $p = 0.392499$ $a = 118.294929$ $b = 11.632513$	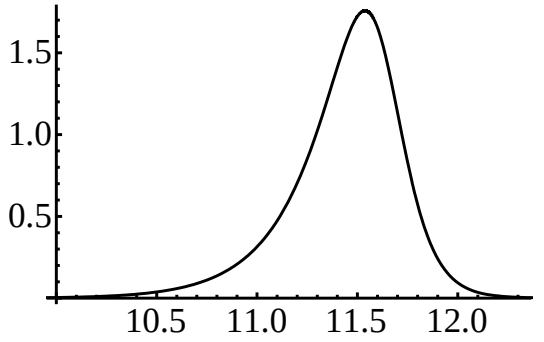
3	$\gamma_3 = 3$ $\gamma_4 = 60$ $\lambda_2 = 0.143831$ $\tau_3 = 0.211153$ $\tau_4 = 0.203575$ $p = 0.820405$ $a = 4.453323$ $b = 0.594326$	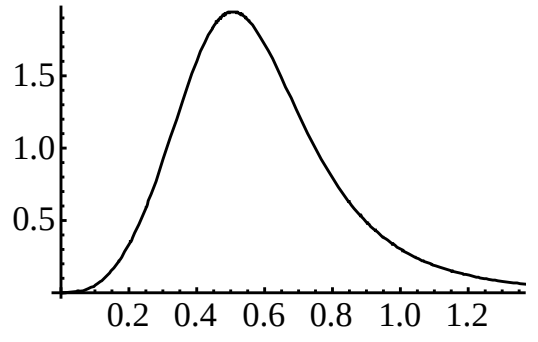
4	$\gamma_3 = 4$ $\gamma_4 = 400$ $\lambda_2 = 0.139097$ $\tau_3 = 0.243899$ $\tau_4 = 0.216258$ $p = 0.984940$ $a = 4.084208$ $b = 0.514413$	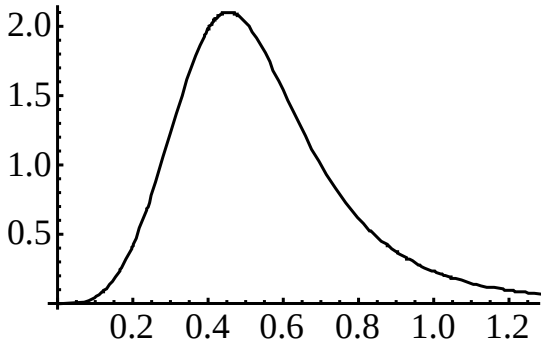

Figure 2: Four asymmetric Dagum distributions with their conventional moment-based parameters of skew (γ_3) and kurtosis (γ_4), L-moment-based parameters of L-scale (λ_2), L-skew (τ_3), and L-kurtosis (τ_4), and corresponding shape and scale parameters p, a, and b for equation (2). Note that the standard deviation for each distribution is $\sigma = 1/\sqrt{12}$.

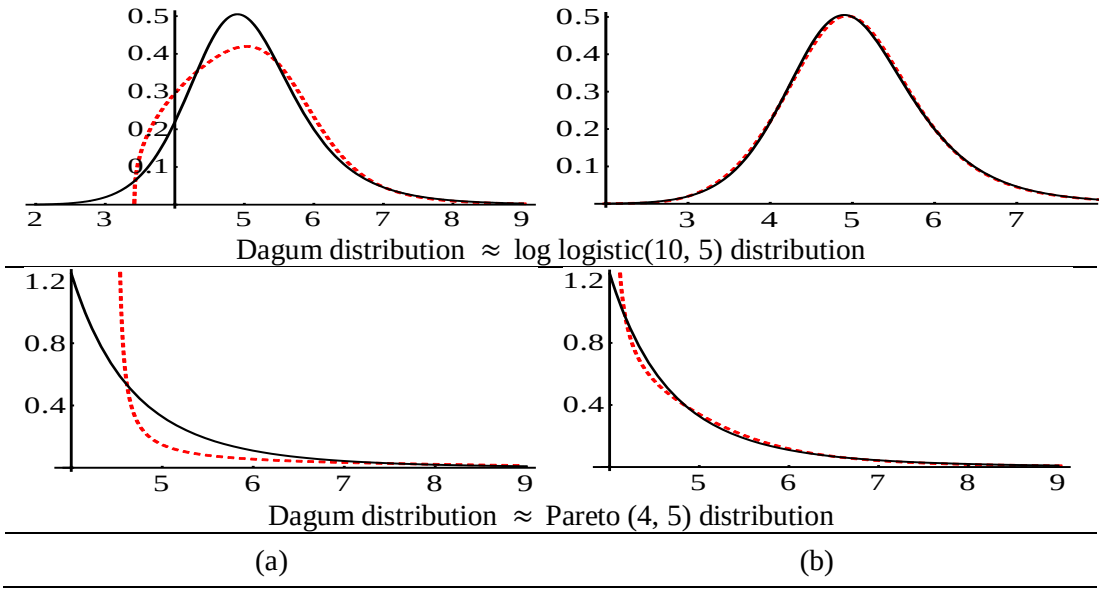

Figure 3: The pdfs of the two distributions, namely, log logistic (10, 5) and Pareto (4, 5) superimposed by the pdfs (dashed curves) of (a) conventional moment- and (b) L-moment-based Dagum distributions.

The results in Tables 6 and 7 demonstrate that L-moment-based estimators are superior to their conventional moment-based counterparts in terms of both smaller relative bias and error. Further, these advantages are most pronounced in the context of smaller sample sizes and higher-order moments. For example, for distribution 4, given a sample of size $n = 25$, the conventional moment-based estimates (g_3 and g_4) generated in the simulation were, on average, 29.85% and 0.51% of their corresponding parameters (γ_3 and γ_4). On the other hand, for the same distribution, the L-moment-based estimates (t_3 and t_4) generated in the simulation were, on average, 90.49% and 93.44% of their corresponding parameters (τ_3 and τ_4). Thus, the relative biases of the estimators based on L-moments are essentially negligible compared to those associated with the estimators based on conventional moments. Furthermore, it can be verified that the (relative) standard errors associated with the estimates t_3 and t_4 are relatively much smaller and more stable than the (relative) standard errors associated with the estimates g_3 and g_4.

3.2 Distribution Fitting

3.2.1 Theoretical distributions

Given in Figure 3 are the pdfs of log-logistic (10, 5) and Pareto (4, 5) distributions superimposed by the pdfs (dashed curves) of Dagum distributions in both (a) conventional moment- and (b) L-moment-based systems. The conventional moment-based parameters of standard deviation (σ), skew (γ_3), and kurtosis (γ_4) associated with log-logistic (10, 5) and Pareto (4, 5) distributions—given in Table 4—were computed by using equations (A.3)−(A.5) in the Appendix. The values of the shape and scale parameters (p, a, and b) were determined by solving equations (A.7)—(A.9) from the Appendix using moment

matching technique. The solved values of p, a, and b were used in (3) to superimpose the conventional moment-based Dagum distribution as shown in Figure 3 (a).

The L-moment-based parameters of L-scale (λ_2), L-skew (τ_3), and L-kurtosis (τ_4) associated with the two distributions in Figure 3, given in Table 5, were obtained in three steps as: (a) compute the values of PWMs $(\beta_{r=0,1,2,3})$ using (4), (b) substitute these PWMs into (5)−(8) to obtain the values of the first four L-moments, and (c) compute the values of τ_3 and τ_4 using $\tau_3 = \lambda_3/\lambda_2$ and $\tau_4 = \lambda_4/\lambda_2$. The values of shape and scale parameters (p, a, and b) given in Table 5 were determined by solving the systems of equations (15)−(17). These values of p, a, and b were used in (3) to superimpose the L-moment-based Dagum distributions as shown in Figure 3 (b).

To superimpose the Dagum distribution the quantile function $q(u)$ in (2) was transformed as: (a) $\left(\bar{X}\sigma - \mu S + Sq(u)\right) / \sigma$, and (b) $\left(\ell_1\lambda_2 - \lambda_1\ell_2 + \ell_2 q(u)\right)/\lambda_2$, respectively, where $(\bar{X},\ S)$ and $(\mu,\ \sigma)$ are the values of (mean, standard deviation), whereas $(\ell_1,\ \ell_2)$ and $(\lambda_1,\ \lambda_2)$ are the values of (L-mean, L-scale) obtained from the original distribution and the Dagum distribution, respectively.

Inspection of the graphs in Figure 3 (a) and (b) indicate that the L-moment-based Dagum pdfs provide a more accurate approximation of the two distributions than those based on conventional moment theory.

3.2.2 Empirical distributions

Figure 4 gives the conventional moment- and the L-moment-based Dagum pdfs superimposed on the histogram of poverty rate of 5- to 17-year olds data obtained from $n = 533$ school districts with more than 15,000 students (http://nces.ed.gov/programs/digest/d11/tables/dt11_096.asp) in the U.S.

The conventional moment-based estimates $(S, g_3, \text{and } g_4)$ of standard deviation, skew, and kurtosis $(\sigma, \gamma_3, \text{and } \gamma_4)$ and the L-moment-based estimates $(\ell_2, t_3, \text{and } t_4)$ of L-scale, L-skew, and L-kurtosis $(\lambda_2, \tau_3, \text{and } \tau_4)$ were computed for the sample of size $n = 533$. The estimates of σ, $\gamma_3, \text{and } \gamma_4$ were computed based on Fisher's k-statistics formulae [16, pp. 47-48], whereas the estimates of $\lambda_2, \tau_3, \text{and } \tau_4$ were computed using (5)−(8) and (10), respectively. These sample estimates were then used to solve for the values of shape and scale parameters (p, a, and b) using (a) equations (A.7)−(A.9) in the Appendix and (b) equations (15) − (17). The solved values of p, a, and b were subsequently used in (3) to superimpose the pdfs of the Dagum distributions as shown in Figure 4 (a) and (b).

Inspection of the two panels in Figure 4 demonstrates that the L-moment-based Dagum pdf provides a better fit to the sample data. The chi-square goodness of fit statistics along with their corresponding p-values given in Table 3 provide evidence that the conventional moment-based Dagum distribution does not provide a good fit to the actual data, whereas, the L-moment-based Dagum distribution fits very well. Note that the degrees of freedom for the chi-square goodness of fit tests were computed as df = 8 = 12 (class intervals) – 3 (parameter estimates) – 1 (sample size).

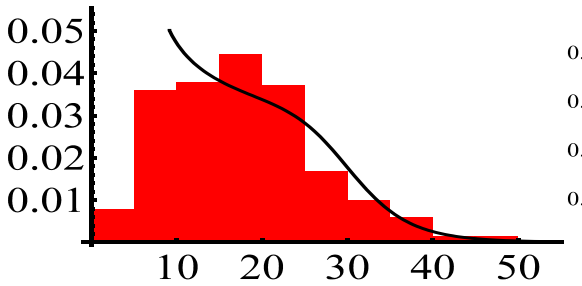

Conventional moment-based Dagum distribution superimposed on the histogram of the Poverty rate of 5- to 17-year olds data

Estimates	Shape parameters
$\bar{X} = 17.7105$	$p = 0.103878$
$S = 0.0108$	$a = 7.225442$
$g_3 = 0.7979$	$b = 0.838858$
$g_4 = 0.7262$	

(a)

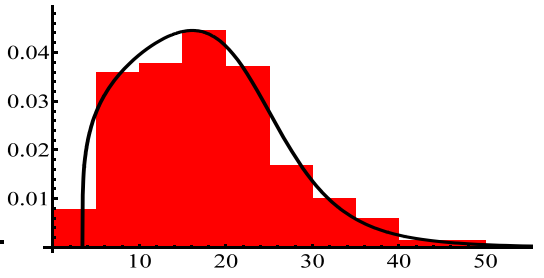

L-moment-based Dagum distribution superimposed on the histogram of the Poverty rate of 5- to 17-year olds data

Estimates	Shape parameters
$\ell_1 = 17.7105$	$p = 0.229529$
$\ell_2 = 4.8776$	$a = 5.443231$
$t_3 = 0.1333$	$b = 0.788525$
$t_4 = 0.1205$	

(b)

Figure 4: Histograms of the Poverty rate of 5- to 17-year olds $(n = 533)$ data superimposed by (a) conventional moment- and (b) L-moment-based Dagum distributions. To superimpose the Dagum distribution (curves), the quantile function $q(u)$ from (2) was transformed as (a) $\left(\bar{X}\sigma - \mu S + Sq(u)\right) / \sigma$, and (b) $\left(\ell_1\lambda_2 - \lambda_1\ell_2 + \ell_2 q(u)\right)/\lambda_2$, respectively, where $(\bar{X},\ S)$ and $(\mu,\ \sigma)$ are the values of (mean, standard deviation), whereas $(\ell_1,\ \ell_2)$ and $(\lambda_1,\ \lambda_2)$ are the values of (L-mean, L-scale) obtained from the actual data and the Dagum distributions, respectively.

Table 3: Chi-square goodness of fit statistics for the conventional (C) moment- and L-moment- (L) based Dagum approximations for the Poverty rate of 5- to 17-year olds data $(n = 533)$ in Figure 3.

%	Exp.	Obs. (C)	Obs. (L)	Poverty rate (C)	Poverty rate (L)
5	26.65	42	29	< 6.6399	< 5.5054
10	26.65	12	21	$6.6399 - 7.3568$	$5.5054 - 7.0613$
20	53.30	39	64	$7.3568 - 9.1622$	$7.0613 - 9.7721$
30	53.30	48	48	$9.1622 - 11.3074$	$9.7721 - 12.2194$
40	53.30	53	49	$11.3074 - 13.7083$	$12.2194 - 14.5284$
50	53.30	58	54	$13.7083 - 16.3206$	$14.5284 - 16.7800$
60	53.30	66	52	$16.3206 - 19.1232$	$16.7800 - 19.0649$
70	53.30	73	65	$19.1232 - 22.1331$	$19.0649 - 21.5265$
80	53.30	52	49	$22.1331 - 25.4843$	$21.5265 - 24.4704$
90	53.30	38	44	$25.4843 - 29.8106$	$24.4704 - 28.8924$
95	26.65	19	24	$29.8106 - 33.3668$	$28.8924 - 33.1684$
100	26.65	33	34	33.3668 or more	33.1684 or more
				$\chi^2 = 40.11$	$\chi^2 = 11.30$
				$p < 0.001$	$p = 0.185$

Table 4: Conventional moment-based parameters of mean (μ), standard deviation (σ), skew (γ_3), and kurtosis (γ_4) along with their corresponding values of shape and scale parameters $(p,\ a,$ and $b)$ for the two distributions (dashed curves) in Figure 2 (a).

Dist.	μ	σ	γ_3	γ_4	p	a	b
1	1.665666	0.940757	0.936674	3.510210	0.234928	6.021672	2.378523
2	0.511138	1.290994	4.647580	70.8	0.021685	4.351457	5.388546

Table 5: L-moment based parameters of L-mean (λ_1), L-scale (λ_2), L-skew (τ_3), and L-kurtosis (τ_4) along with their corresponding values of shape and scale parameters $(p,$ $a,$ and $b)$ for the two distributions (dashed curves) in Figure 2 (b).

Dist.	λ_1	λ_2	τ_3	τ_4	p	a	b
1	3.230377	0.508320	0.1	0.1750	0.677402	7.264128	3.413678
2	0.953430	0.555556	0.428571	0.248120	0.224958	2.596406	1.810060

Table 6: Skew (γ_3) and Kurtosis (γ_4) results for the Conventional moment procedure.

Dist.	Parameter	Estimate	95% Bootstrap C.I.	St. Error	RB%
		$n = 25$			
1	$\gamma_3 = -0.5$	$g_3 = -0.3618$	$-0.3695, -0.3541$	0.00391	-27.64
	$\gamma_4 = 1.5$	$g_4 = 0.4887$	$0.4725, 0.5062$	0.00856	-67.42
2	$\gamma_3 = -1.0$	$g_3 = -0.6842$	$-0.6922, -0.6761$	0.00414	-31.58
	$\gamma_4 = 2.5$	$g_4 = 0.7952$	$0.7721, 0.8165$	0.01132	-68.19
3	$\gamma_3 = 3.0$	$g_3 = 1.054$	$1.0437, 1.0641$	0.00521	-64.97
	$\gamma_4 = 60$	$g_4 = 1.7$	$1.6631, 1.7381$	0.01919	-97.17
4	$\gamma_3 = 4.0$	$g_3 = 1.194$	$1.1835, 1.2050$	0.00547	-70.15
	$\gamma_4 = 400$	$g_4 = 2.059$	$2.0170, 2.0990$	0.02090	-99.49
		$n = 1000$			
1	$\gamma_3 = -0.5$	$g_3 = -0.4963$	$-0.4982, -0.4944$	0.00948	-0.13
	$\gamma_4 = 1.5$	$g_4 = 1.465$	$1.4583, 1.4723$	0.00354	-2.33
2	$\gamma_3 = -1.0$	$g_3 = -0.9893$	$-0.9916, -0.9873$	0.00108	-2.38
	$\gamma_4 = 2.5$	$g_4 = 2.421$	$2.4076, 2.4338$	0.00662	-3.16
3	$\gamma_3 = 3.0$	$g_3 = 2.444$	$2.4261, 2.4604$	0.00867	-18.53
	$\gamma_4 = 60$	$g_4 = 16.78$	$16.4370, 17.1737$	0.18740	-72.03
4	$\gamma_3 = 4.0$	$g_3 = 2.969$	$2.9484, 2.9921$	0.01111	-25.78
	$\gamma_4 = 400$	$g_4 = 23.58$	$23.0814, 24.1082$	0.2598	-94.11

Table 7: L-skew (τ_3) and L-kurtosis (τ_4) results for the L-moment procedure.

Dist.	Parameter	Estimate	95% Bootstrap C.I.	St. Error	RB%
		$n = 25$			
1	$\tau_3 = -0.0751$	$t_3 = -0.0719$	$-0.0733, -0.0705$	0.00071	-4.26
	$\tau_4 = 0.1727$	$t_4 = 0.1710$	$0.1700, 0.1720$	0.00051	-0.98
2	$\tau_3 = -0.1424$	$t_3 = -0.1361$	$-0.1375, -0.1347$	0.00071	-4.42
	$\tau_4 = 0.1788$	$t_4 = 0.1768$	$0.1758, 0.1779$	0.00054	-1.12
3	$\tau_3 = 0.2112$	$t_3 = 0.1918$	$0.1899, 0.1932$	0.00080	-9.19
	$\tau_4 = 0.2036$	$t_4 = 0.1924$	$0.1911, 0.1937$	0.00066	-5.50
4	$\tau_3 = 0.2439$	$t_3 = 0.2207$	$0.2191, 0.2223$	0.00082	-9.51
	$\tau_4 = 0.2163$	$t_4 = 0.2021$	$0.2008, 0.2036$	0.00070	-6.56
		$n = 1000$			
1	$\tau_3 = -0.0751$	$t_3 = -0.0749$	$-0.0752, -0.0747$	0.00011	-----
	$\tau_4 = 0.1727$	$t_4 = 0.1726$	$0.1724, 0.1727$	0.00007	-----
2	$\tau_3 = -0.1424$	$t_3 = -0.1419$	$-0.1421, -0.1417$	0.00011	-0.35
	$\tau_4 = 0.1788$	$t_4 = 0.1787$	$0.1785, 0.1788$	0.00008	-----
3	$\tau_3 = 0.2112$	$t_3 = 0.2104$	$0.2102, 0.2107$	0.00014	-0.38
	$\tau_4 = 0.2036$	$t_4 = 0.2031$	$0.2029, 0.2033$	0.00012	-0.25
4	$\tau_3 = 0.2439$	$t_3 = 0.2432$	$0.2430, 0.2435$	0.00015	-0.29
	$\tau_4 = 0.2163$	$t_4 = 0.2159$	$0.2157, 0.2162$	0.00013	-0.18

4 *L*-Correlations for the Dagum Distributions

Let Y_j and Y_k be random variables with cdfs $F(Y_j)$ and $F(Y_k)$ respectively. The second L-moments of Y_j and Y_k can alternatively be defined as [19]

$$\lambda_2(Y_j) = 2Cov\left(Y_j, F(Y_j)\right) \tag{19}$$

$$\lambda_2(Y_k) = 2Cov\left(Y_k, F(Y_k)\right) \tag{20}$$

The second L-comoment of Y_j toward Y_k and Y_k toward Y_j are given as

$$\lambda_2(Y_j, Y_k) = 2Cov\left(Y_j, F(Y_k)\right) \tag{21}$$

$$\lambda_2(Y_k, Y_j) = 2Cov\left(Y_k, F(Y_j)\right) \tag{22}$$

The L-correlations of Y_j toward Y_k and Y_k toward Y_j are subsequently defined as:

$$\eta_{jk} = \frac{\lambda_2(Y_j, Y_k)}{\lambda_2(Y_j)} \tag{23}$$

$$\eta_{kj} = \frac{\lambda_2(Y_k, Y_j)}{\lambda_2(Y_k)} \tag{24}$$

The L-correlation given in (23) (or, 24) is bounded in the interval $-1 \leq \eta_{jk} \leq 1$. A

value of $\eta_{jk} = 1$ $(\eta_{jk} = -1)$ implies that Y_j and Y_k have a strictly and monotonically increasing (decreasing) relationship. See Serfling and Xiao [19] for further details on the topics related to the L-correlation.

The extension of the Dagum distributions to multivariate data generation can be achieved by specifying T quantile functions as given in (2) with a specified L-correlation structure. Specifically, let $Z_1, \ldots, Z_T$ denote standard normal variables with cdfs and the joint pdf associated with Z_j and Z_k given by the following expressions:

$$\Phi(Z_j) = \int_{-\infty}^{z_j} (2\pi)^{-1/2} \exp\{-v_j^2/2\}\, dv_j \tag{25}$$

$$\Phi(Z_k) = \int_{-\infty}^{z_k} (2\pi)^{-1/2} \exp\{-v_k^2/2\}\, dv_k \tag{26}$$

$$f_{jk} = \left(2\pi\left(1 - r_{jk}^2\right)^{1/2}\right)^{-1} \exp\left\{-\left(2\left(1 - r_{jk}^2\right)\right)^{-1} \left(z_j^2 + z_k^2 - 2r_{jk}\, z_j\, z_k\right)\right\}. \tag{27}$$

where r_{jk} in (27) is the intermediate Pearson correlation (IC) between Z_j and Z_k. Using the cdfs in (25) and (26) as zero-one uniform deviates, i.e., $\Phi(Z_j), \Phi(Z_k) \sim U(0,1)$, the quantile function defined in (2) can be expressed as a function of $\Phi(Z_j)$, or $\Phi(Z_k)$ $\left(\text{e.g., } q_j\left(\Phi(Z_j)\right) \text{ or } q_k\left(\Phi(Z_k)\right)\right)$. Thus, the L-correlation of $Y_j = q_j\left(\Phi(Z_j)\right)$ toward $Y_k = q_k\left(\Phi(Z_k)\right)$ can be determined using (23) with the denominator standardized to $\lambda_2(Y_j) = 1/\sqrt{\pi}$ for the standard normal distribution as

$$\eta_{jk} = 2\sqrt{\pi} \int_{-\infty}^{\infty} \int_{-\infty}^{\infty} x_j\left(q_j\left(\Phi(Z_j)\right)\right) \Phi(z_k)\, f_{jk}\, dz_j\, dz_k. \tag{28}$$

The variable $x_j\left(q_j\left(\Phi(Z_j)\right)\right)$ in (28) is the standardized quantile function of (2) such that it has a mean of zero and L-scale equal to $\lambda_2 = 1/\sqrt{\pi}$. That is, the quantile function $Y_j = q_j\left(\Phi(Z_j)\right)$ is standardized by a linear transformation as:

$$x_j\left(q_j\left(\Phi(Z_j)\right)\right) = \delta\left(q_j\left(\Phi(Z_j)\right) - \lambda_1\right) \tag{29}$$

where λ_1 is the mean from (14) and δ is a constant that scales λ_2 in (15) and in the denominator of (23) to $1/\sqrt{\pi}$. Specifically, the constant δ for the Dagum family of distributions can be expressed as:

$$\delta = \frac{-\Gamma[p]\Gamma[2p]}{b\sqrt{\pi}\{\Gamma[1-1/a](\Gamma[2p]\Gamma[p+1/a] - \Gamma[p]\Gamma[2p+1/a])\}}. \tag{30}$$

The next step is to use (28) to solve for the values of the $T(T-1)/2$ ICs (r_{jk}) such that the T specified Dagum distributions have their specified L-correlation structure.

Analogously, the L-correlation of $Y_k = q_k\left(\Phi(Z_k)\right)$ toward $Y_j = q_j\left(\Phi(Z_j)\right)$ is given as:

$$\eta_{kj} = 2\sqrt{\pi}\int_{-\infty}^{\infty}\int_{-\infty}^{\infty} x_k\left(q_k\left(\Phi(Z_k)\right)\right)\Phi(z_j)\, f_{jk}\, dz_k\, dz_j. \tag{31}$$

Note that in general, the L-correlation of $Y_j = q_j\left(\Phi(Z_j)\right)$ toward $Y_k = q_k\left(\Phi(Z_k)\right)$ in (28) is not equal to the L-correlation of $Y_k = q_k\left(\Phi(Z_k)\right)$ toward $Y_j = q_j\left(\Phi(Z_j)\right)$ in (31). These L-correlations are equal only when the values of shape and scale parameters p, a, and b associated with $q_j\left(\Phi(Z_j)\right)$ and $q_k\left(\Phi(Z_k)\right)$ are equal (i.e., when the two distributions are the same). Provided in Algorithm 1 is a source code written in Mathematica [21], which shows an example for computing ICs (r_{jk}) for the L-correlation procedure. The steps for simulating correlated Dagum distributions with specified values of L-skew (τ_3), L-kurtosis (τ_4), and with specified L-correlation structure are given in Section 5.

5 Monte Carlo Simulation with an Example

The procedure for simulating Dagum distributions with specified L-moments and L-correlations can be summarized in the following six steps:

1. Specify the L-moments for T transformations of the form in (2), i.e., $q_1(\Phi(z_1))\ , \dots, q_T(\Phi(z_T))$ and obtain the solutions for the shape and scale parameters p, a, and b by simultaneously solving the systems of equations (15)−(17) for the specified values of L-scale (λ_2), L-skew (τ_3), and L-kurtosis (τ_4) for each distribution. Specify a $T \times T$ matrix of L-correlations (η_{jk}) for $q_j\left(\Phi(z_j)\right)$ toward $q_k\left(\Phi(Z_k)\right)$, where $j < k \in \{1, 2, \dots, T\}$.
2. Compute the values of intermediate (Pearson) correlations (ICs), r_{jk}, by substituting the value of specified L-correlation (η_{jk}) and the solved values of p, a, and b from Step 1 into the left- and the right-hand sides of (28), respectively, and then numerically integrating (28) to solve for r_{jk}. See Algorithm 1 for an example. Repeat this step separately for all $T(T-1)/2$ pairwise combinations of ICs.
3. Assemble the ICs computed in Step 2 into a $T \times T$ matrix and then decompose this matrix using Cholesky factorization. Note that this step requires the IC matrix to be positive definite.
4. Use elements of the matrix resulting from Cholesky factorization of Step 3 to generate T standard normal variables $(Z_1, \dots, Z_T)$ correlated at the IC levels as follows:

$$\begin{aligned}
Z_1 &= a_{11}V_1 \\
Z_2 &= a_{12}V_1 + a_{22}V_2 \\
&\vdots \\
Z_j &= a_{1j}V_1 + a_{2j}V_2 + \cdots + a_{ij}V_i + \cdots + a_{jj}V_j \\
&\vdots \\
Z_T &= a_{1T}V_1 + a_{2T}V_2 + \cdots + a_{iT}V_i + \cdots + a_{jT}V_T + \cdots + a_{TT}V_T
\end{aligned} \tag{32}$$

where $V_1, \dots, V_T$ are independent standard normal random variables and where a_{ij} is the element in the i-th row and j-th column of the matrix resulting from Cholesky

factorization of Step 3.

5. Substitute $Z_1, \ldots, Z_T$ from Step 4 into the following Taylor series-based expansion for computing the cdf, $\Phi(Z_j)$, of standard normal distribution [17]:

$$\Phi(Z_j) = \left(\frac{1}{2}\right) + \phi(Z_j)\left\{Z_j + \frac{Z_j^3}{3} + \frac{Z_j^5}{(3\cdot 5)} + \frac{Z_j^7}{(3\cdot 5\cdot 7)} + \cdots\right\} \tag{33}$$

where $\phi(Z_j)$ is the pdf of standard normal distribution and the absolute error associated with (33) is less than 8×10^{-16}.

6. Substitute the uniform (0, 1) variables, $\Phi(Z_j)$, generated in Step 5 into the T equations of the form $q_j(\Phi(z_j))$ in (2) to generate the Dagum distributions with specified values of L-skew (τ_3), L-kurtosis (τ_4), and with specified L-correlation structure.

For the purpose of evaluating the proposed methodology and demonstrating the steps above, an example is subsequently provided to compare the L-correlation-based procedure with the conventional product moment-based (Pearson) correlation procedure. Specifically, the distributions in Figure 2 are used as a basis for a comparison using the specified correlation matrix in Table 8. Let the four distributions in Figure 2 be $Y_1 = q_1(\Phi(Z_1))$, $Y_2 = q_2(\Phi(Z_2))$, $Y_3 = q_3(\Phi(Z_3))$, and $Y_4 = q_4(\Phi(Z_4))$, obtained from the quantile functions from (2). Presented in Tables 9 and 10 are the intermediate correlations (ICs) obtained for the conventional product moment-based (Pearson) correlation and L-moment-based L-correlation procedures, respectively, for the distributions in Figure 2. Provided in Algorithm 2 is a source code written in Mathematica [21], which shows an example for computing ICs (r_{jk}) for the conventional product moment-based (Pearson) correlation procedure. Provided in Tables 11 and 12 are the results of Cholesky factorization on the IC matrices in Tables 9 and 10, respectively. The elements of matrices in Tables 11 and 12 are used to generate $Z_1, \ldots, Z_4$ correlated at the IC levels by making use of the formulae (32) in Step 4 with $T = 4$. The values of $Z_1, \ldots, Z_4$ are then used in (33) to obtain the Taylor series-based approximations of the cdfs $\Phi(Z_1)$, $\Phi(Z_2)$, $\Phi(Z_3)$, and $\Phi(Z_4)$, which are treated as uniform $(0, 1)$ variables. These uniform variables are used in (2) to obtain the quantile functions $q_1(\Phi(Z_1))$, $q_2(\Phi(Z_2))$, $q_3(\Phi(Z_3))$, and $q_4(\Phi(Z_4))$ to generate the four distributions in Figure 2 that are correlated at the specified correlation level of Table 8.

For the Monte Carlo simulation, a Fortran [18] algorithm was written for both procedures to generate 25,000 independent sample estimates for the specified parameters of (a) conventional product moment-based (Pearson) correlation (ρ_{jk}), and (b) L-moment-based L-correlation (η_{jk}) based on samples of sizes $n = 25$ and $n = 1000$. The estimate for ρ_{jk} was based on the usual formula for the Pearson correlation statistic. The estimate of η_{jk} was computed by substituting (19) and (21) into (23), where the empirical forms of the cdfs were used in (19) and (21). The sample estimates ρ_{jk} and η_{jk} were both transformed using Fisher's z' transformations. Bias-corrected accelerated bootstrapped average estimates (Estimate), 95% bootstrap confidence intervals (95% Bootstrap C.I.), and standard errors (St. Error) were obtained for the estimates associated with the parameters $\left(z'_{(\rho_{jk})} \text{ and } z'_{(\eta_{jk})}\right)$ using 10,000 resamples via

the commercial software package Spotfire S+ [20]. The bootstrap results associated with the estimates of $z'_{(\rho_{jk})}$ and $z'_{(\eta_{jk})}$ were transformed back to their original metrics. Further, if a parameter was outside its associated 95% bootstrap C.I., then the percentage of relative bias (RB%) was computed for the estimate as in (18). The results of this simulation are presented in Tables 13 and 14, and are discussed in Section 6.

Table 8: Specified correlation matrix for the conventional moment- and *L*-moment-based procedures for the four distributions in Figure 2.

Dist.	1	2	3	4
1	1.00			
2	0.85	1.00		
3	0.80	0.75	1.00	
4	0.70	0.70	0.75	1.00

Table 9: Intermediate correlation matrix for the conventional moment-based procedure for the four distributions in Figure 2.

Dist.	1	2	3	4
1	1.00			
2	0.858484	1.00		
3	0.891443	0.873067	1.00	
4	0.802731	0.841130	0.791261	1.00

Table 10: Intermediate correlation matrix for the *L*-moment-based procedure for the four distributions in Figure 2.

Dist.	1	2	3	4
1	1.00			
2	0.844768	1.00		
3	0.793668	0.742009	1.00	
4	0.692277	0.691379	0.737035	1.00

Table 11: Matrix obtained from Cholesky factorization of the intermediate correlation matrix in Table 9.

$a_{11} = 1.00$	$a_{12} = 0.858484$	$a_{13} = 0.891443$	$a_{14} = 0.802731$
$a_{21} = 0.00$	$a_{22} = 0.512841$	$a_{23} = 0.210157$	$a_{24} = 0.296384$
$a_{31} = 0.00$	$a_{32} = 0.00$	$a_{33} = 0.401451$	$a_{34} = 0.033341$
$a_{41} = 0.00$	$a_{42} = 0.00$	$a_{43} = 0.00$	$a_{44} = 0.516398$

Table 12: Matrix obtained from Cholesky factorization of the intermediate correlation matrix in Table 10.

$a_{11} = 1.00$	$a_{12} = 0.844768$	$a_{13} = 0.793668$	$a_{14} = 0.692277$
$a_{21} = 0.00$	$a_{22} = 0.535133$	$a_{23} = 0.133693$	$a_{24} = 0.199139$
$a_{31} = 0.00$	$a_{32} = 0.00$	$a_{33} = 0.593479$	$a_{34} = 0.271237$
$a_{41} = 0.00$	$a_{42} = 0.00$	$a_{43} = 0.00$	$a_{44} = 0.638378$

6 Discussion and Conclusion

One of the advantages that L-moments have over conventional moments can be expressed in the context of estimation. The L-moment-based estimators of L-skew and L-kurtosis can be far less biased than the conventional moment-based estimators of skew and kurtosis when samples are drawn from the distributions with more severe departures from normality [3, 4-7, 9-11, 15, 19]. Inspection of the simulation results in Tables 6 and 7 clearly indicates that this is the case for the Dagum distributions. That is, the superiority that estimates of L-moment ratios (τ_3 and τ_4) have over their corresponding conventional moment-based estimates of skew and kurtosis (γ_3 and γ_4) is obvious. For example, for samples of size $n = 25$, the estimates of γ_3 and γ_4 for distribution 4 were, on average, 29.85% and 0.51% of their associated parameters, whereas the estimates of τ_3 and τ_4 were 90.49% and 93.44% of their associated parameters. This advantage of L-moment-based estimates can also be expressed by comparing their relative standard errors (RSEs), where $\text{RSE} = \{(\text{St.Error}/\text{Estimate}) \times 100\}$. Comparing Tables 6 and 7, it is evident that the estimates of τ_3 and τ_4 are more efficient as their RSEs are considerably smaller than the RSEs associated with the conventional moment-based estimates of γ_3 and γ_4. For example, in terms of distribution 4 in Figure 2, inspection of Tables 6 and 7 (for $n = 1000$), indicates that RSE measures of: $\text{RSE}(t_3) = 0.061\%$ and $\text{RSE}(t_4) = 0.060\%$ are considerably smaller than the RSE measures of: $\text{RSE}(g_3) = 0.374\%$ and $\text{RSE}(g_4) = 1.102\%$. This demonstrates that the estimates of L-skew and L-kurtosis have more precision because they have less variance around their bootstrapped estimates.

Another advantage of L-moments can be highlighted in the context of distribution fitting.

Comparison of the two distributions in Figure 3 (a) and (b) clearly indicates that L-moment-based Dagum distributions provide a better fit to the theoretical distributions compared with their conventional moment-based counterparts. In the context of fitting real-world data, the L-moment-based Dagum distribution in Figure 4 (b) provides a better fit to the Poverty rate of 5- to 17-year olds ($n = 533$) data than the conventional moment-based Dagum distribution in Figure 4 (a).

Presented in Tables 13 and 14 are the simulation results of conventional product moment-based (Pearson) correlations and L-moment-based L-correlations, respectively. Overall inspection of these tables indicates that the L-correlation is superior to Pearson correlation in terms of relative bias. For example, for $n = 25$, the percentage of relative bias for the two distributions, distribution 2 and distribution 4, in Figure 2 was 9.10% for the Pearson correlation compared with only 1.12% for the L-correlation. It is also noted that the variability associated with bootstrapped estimates of L-correlation appears to be more stable than that of the bootstrapped estimates of Pearson correlation both within and across different conditions.

In summary, the new L-moment-based procedure is an attractive alternative to the more traditional conventional moment-based procedure in the context of Dagum distributions. In particular, the L-moment-based procedure has distinct advantages when distributions with large departures from normality are used. Finally, we note that Mathematica [21] source codes are available from the authors for implementing both the conventional moment- and L-moment-based procedures.

Table 13: Correlation results for the Conventional moment procedure

A. $n = 25$

Parameter	Estimate	95% Bootstrap C.I.	St. Error	RB%
$\rho_{12} = 0.85$	0.8578	$(0.8571, 0.8586)$	0.00141	0.92
$\rho_{13} = 0.80$	0.8440	$(0.8433, 0.8446)$	0.00111	5.50
$\rho_{14} = 0.70$	0.7531	$(0.7521, 0.7541)$	0.00115	7.59
$\rho_{23} = 0.75$	0.8037	$(0.8031, 0.8046)$	0.00104	7.16
$\rho_{24} = 0.70$	0.7637	$(0.7629, 0.7647)$	0.00105	9.10
$\rho_{34} = 0.75$	0.7849	$(0.7837, 0.7863)$	0.00174	4.65

B. $n = 1000$

Parameter	Estimate	95% Bootstrap C.I.	St. Error	RB%
$\rho_{12} = 0.85$	0.8500	$(0.8499, 0.8502)$	0.00022	-----
$\rho_{13} = 0.80$	0.8055	$(0.8052, 0.8058)$	0.00038	0.69
$\rho_{14} = 0.70$	0.7073	$(0.7070, 0.7076)$	0.00034	1.04
$\rho_{23} = 0.75$	0.7559	$(0.7556, 0.7562)$	0.00034	0.79
$\rho_{24} = 0.70$	0.7081	$(0.7077, 0.7085)$	0.00037	1.16
$\rho_{34} = 0.75$	0.7551	$(0.7547, 0.7555)$	0.00043	0.68

Table 14: Correlation results for the L-moment procedure.

A. $n = 25$

Parameter	Estimate	95% Bootstrap C.I.	St. Error	RB%
$\eta_{12} = 0.85$	0.8565	$(0.8556, 0.8572)$	0.00149	0.76
$\eta_{13} = 0.80$	0.8072	$(0.8061, 0.8081)$	0.00147	0.90
$\eta_{14} = 0.70$	0.7087	$(0.7072, 0.7101)$	0.00147	1.24
$\eta_{23} = 0.75$	0.7584	$(0.7572, 0.7596)$	0.00148	1.12
$\eta_{24} = 0.70$	0.7078	$(0.7064, 0.7093)$	0.00148	1.12
$\eta_{34} = 0.75$	0.7560	$(0.7547, 0.7573)$	0.00152	0.80

B. $n = 1000$

Parameter	Estimate	95% Bootstrap C.I.	St. Error	RB%
$\eta_{12} = 0.85$	0.8500	$(0.8499, 0.8501)$	0.00021	-----
$\eta_{13} = 0.80$	0.8001	$(0.7999, 0.8002)$	0.00021	-----
$\eta_{14} = 0.70$	0.7002	$(0.6999, 0.7004)$	0.00021	-----
$\eta_{23} = 0.75$	0.7500	$(0.7498, 0.7502)$	0.00021	-----
$\eta_{24} = 0.70$	0.7001	$(0.6998, 0.7003)$	0.00022	-----
$\eta_{34} = 0.75$	0.7500	$(0.7498, 0.7502)$	0.00023	-----

(* Intermediate Correlation *)
$r_{12} = 0.844768;$

Needs[“MultivariateStatistics`”]
f_{12} = PDF[MultinormalDistribution[{0, 0}, {{1, r_{12}}, {r_{12}, 1}}], {Z_1, Z_2}];
Φ_1 = CDF[NormalDistribution[0, 1], Z_1];
Φ_2 = CDF[NormalDistribution[0, 1], Z_2];

(* Parameters for distribution 1 in Figure 2 *)
p_1= 0.520053;
a_1= 42.352031;
b_1= 5.136684;

$\lambda_1 = 4.991085;$
$\delta_1 = 3.571456;$

(* Quantile function from equation (2) *)
$y_1 = b_1 * \left({\Phi_1}^{(-1/p_1)} - 1\right)^{(-1/a_1)};$

(* Standardizing constants λ_1 and δ_1 were obtained, respectively, from equations (14) and (30) *)
$x_1 = \delta_1 * (y_1 - \lambda_1);$

(* Compute the specified L-correlation *)
$\eta_{12} = 2\sqrt{\pi} *$ NIntegrate[$x_1 * \Phi_2 * f_{12}$, { Z_1 , -8, 8}, { Z_2 , -8, 8}, Method → “MultiDimensionalRule”]

0.85

Algorithm 1: Mathematica source code for computing intermediate correlations for specified L-correlations. The example is for distribution $j = 1$ toward distribution $k = 2$ (η_{12}). See distributions 1 and 2 in Figure 2, specified correlation in Table 8, and intermediate correlation in Table 10.

```
(* Intermediate Correlation *)
r12 = 0.858484;

Needs["MultivariateStatistics`"]
f12 = PDF[MultinormalDistribution[{0, 0}, {{1, r12}, {r12, 1}}], {Z1, Z2}];
Φ1 = CDF[NormalDistribution[0, 1], Z1];
Φ2 = CDF[NormalDistribution[0, 1], Z2];

(* Parameters for distributions 1 and 2 in Figure 2 *)
p1 = 0.520053;
a1 = 42.352031;
b1 = 5.136684;

p2 = 0.392499;
a2 = 118.294929;
b2 = 11.632513;

(* Quantile functions from equation (2) *)
y1 = b1 * (Φ1^(-1/p1) - 1)^(-1/a1)
y2 = b2 * (Φ2^(-1/p2) - 1)^(-1/a2);
(* Standardizing constants μ1 and μ2 are obtained from equation (A.6) from the
Appendix and σ = 1/√12 *)
x1 = (y1 - μ1)/σ;
x2 = (y2 - μ2)/σ;

(* Compute the specified conventional product moment-based (Pearson) correlation *)
ρ12 = NIntegrate[ x1 * x2 * f12 , { Z1 , - 8, 8}, { Z2 , - 8, 8}, Method →
"MultiDimensionalRule"]

0.85
```

Algorithm 2: Mathematica source code for computing intermediate correlations for specified conventional product moment-based (Pearson) correlations. The example is for distribution $j = 1$ and distribution $k = 2$ (ρ_{12}). See distributions 1 and 2 in Figure 2, specified correlation in Table 8, and intermediate correlation in Table 9.

References

[1] C. Dagum, A model of income distribution and the conditions of existence of moments of finite order, *Proceedings of the 40th Session of the International Statistical Institute*,**46**, (1975), 199–205.

[2] C. Dagum, A new model for personal income distribution: Specification and estimation, *Economie Appliqu´ee*, **30**, (1977), 413–437.

[3] T. C. Headrick, A characterization of power method transformations through *L*-moments, *Journal of Probability and Statistics*, **vol. 2011**, Article ID 497463, 22 pages, (2011). doi:10.1155/2011/497463

[4] T. C. Headrick and M. D. Pant, Simulating non-normal distributions with specified *L*-moments and *L*-correlations, *Statistica Neerlandica*, **66**(4), (2012), 422–441. doi: 10.1111/j.1467-9574.2012.00523.x

[5] T. C. Headrick and M. D. Pant, A method for simulating nonnormal distributions with specified *L*-skew, *L*-kurtosis, and *L*-correlation, *ISRN Applied Mathematics*, **vol. 2012**, Article ID 980827, 23 pages, (2012). doi: 10.5402/2012/980827

[6] T. C. Headrick and M. D. Pant, A logistic *L*-moment-based analog for the Tukey *g-h*, *g*, *h*, and *h-h* system of distributions, *ISRN Probability and Statistics*, **2012**, Article ID 245986, 23 pages, (2012). doi: 10.5402/2012/245986

[7] T. C. Headrick and M. D. Pant, An L -moment-based analog for the Schmeiser-Deutsch class of distributions, *ISRN Applied Mathematics*, **2012**, Article ID 475781, 16 pages, (2012). doi:10.5402/2012/475781

[8] T. C. Headrick, M. D. Pant, and Y. Sheng, On simulating univariate and multivariate Burr Type III and Type XII distributions, *Applied Mathematical Sciences*, **4**(45), (2010), 2207–2240. http://www.m-hikari.com/ams/ams-2010/ams-45-48-2010/index.html

[9] J. R. M. Hosking, L-moments: Analysis and estimation of distributions using linear combinations of order statistics, *Journal of the Royal Statistical Society*, *Series B*, **52**(1), (1990), 105–124.

[10] J. R. M. Hosking, Moments or *L*-moments? An example comparing two measures of distributional shape, *American Statistician*, **46**(3), (1992), 186-189.

[11] J. R. M. Hosking and J. R. Wallis, *Regional frequency analysis: An approach based on L-moments*, Cambridge University Press, Cambridge, UK, 1997.

[12] J. Karvanen and A. Nuutinen, Characterizing the generalized lambda distributions by L-moments, *Computational Statistics & Data Analysis*, **52**, (2008), 1971-1983.

[13] C. Kleiber, A guide to the Dagum distributions, In D. Chotikapanich (Eds.), *Modeling Income Distributions and Lorenz Curves* (pp. 97-117), Springer, 2008.

[14] M. C. Jones, On some expressions for variance, covariance, skewness, and L-moments, *Journal of Statistical Planning and Inference*, **126**(1), (2004), 97-106.

[15] M. D. Pant and T. C. Headrick, A method for simulating Burr Type III and Type XII distributions through *L*-moments and *L*-correlations, *ISRN Applied Mathematics*, **vol. 2013**, Article ID 191604, 14 pages, (2013). doi:10.1155/2013/191604

[16] M. Kendall and A. Stuart, *The advanced theory of statistics*, Fourth edition, Macmillan, New York, 1977.

[17] G. Marsaglia, Evaluating the Normal Distribution, *Journal of Statistical Software*, **11**(5), (2004), 1-10. http://www.jstatsoft.org/v11/i05

[18] Microsoft FORTRAN PowerStation Version 4.0. Microsoft Corporation, USA, 1994.

[19] R. Serfling and P. Xiao, A contribution to multivariate L-moments: L-comoment matrices, *Journal of Multivariate Analysis*, **98**(9), (2007), 1765-1781.
[20] TIBCO Spotfire S+ 8.2.0 for Microsoft Windows. TIBCO Software Inc., Palo Alto, CA, USA, 2010.
[21] Wolfram Mathematica 8.0.4.0 for Microsoft Windows. Wolfram Research, Inc., Champaign, IL, USA, 2011.

Appendix

Conventional Moment-Based System of Equations for Dagum Distributions

The conventional (product) moments associated with Dagum distributions can be obtained from:

$$\mu_r = \int_0^\infty x^r f(x)dx = \frac{b^r \Gamma[1 - r/a]\Gamma[p + r/a]}{\Gamma[p]} \tag{A.1}$$

The mean (μ), standard deviation (σ), skew (γ_3), and kurtosis (γ_4) are defined as in [8]

$$\mu = \mu_1 \tag{A.2}$$
$$\sigma = \sqrt{\mu_2 - \mu_1^2} \tag{A.3}$$
$$\gamma_3 = (\mu_3 - 3\mu_2\mu_1 + 2\mu_1^3)/\sigma^3 \tag{A.4}$$
$$\gamma_4 = (\mu_4 - 4\mu_3\mu_1 - 3\mu_2^2 + 12\mu_2\mu_1^2 - 6\mu_1^4)/\sigma^4. \tag{A.5}$$

In terms of conventional moments, the r-th moment exists only if $a > r$. Suppose that the first four $(r = 4)$ moments exist, then the conventional moment-based mean (μ), standard deviation (σ), skew (γ_3), and kurtosis (γ_4) for the Dagum distribution are obtained using equations (A.1)-(A.5) as:

$$\mu = (b\Gamma[1 - 1/a]\Gamma[p + 1/a])/\Gamma[p] \tag{A.6}$$
$$\sigma = \frac{b\sqrt{(\Gamma[p]\Gamma[1 - 2/a]\Gamma[p + 2/a] - \Gamma[1 - 1/a]^2\Gamma[p + 1/a]^2)}}{\Gamma[p]} \tag{A.7}$$
$$\begin{aligned}\gamma_3 = {} & (2\Gamma[1 - 1/a]^3\Gamma[p + 1/a]^3 + \Gamma[p]^2\Gamma[1 - 3/a]\Gamma[p + 3/a] - \\ & 3\Gamma[p]\Gamma[1 - 1/a]\Gamma[p + 1/a]\Gamma[1 - 2/a]\Gamma[p + 2/a])/ \\ & (\Gamma[p]\Gamma[1 - 2/a]\Gamma[p + 2/a] - \Gamma[1 - 1/a]^2\Gamma[p + 1/a]^2)^{3/2}\end{aligned} \tag{A.8}$$
$$\begin{aligned}\gamma_4 = {} & \{\Gamma[p]^2(\Gamma[p]\Gamma[1 - 4/a]\Gamma[p + 4/a] - 3\Gamma[1 - 2/a]^2\Gamma[p + 2/a]^2) - \\ & 4\Gamma[p]^2\Gamma[1 - 1/a]\Gamma[p + 1/a]\Gamma[1 - 3/a]\Gamma[p + 3/a] + \\ & 12\Gamma[p]\Gamma[1 - 2/a]\Gamma[p + 2/a]\Gamma[1 - 1/a]^2\Gamma[p + 1/a]^2 - \\ & 6\Gamma[1 - 1/a]^4\Gamma[p + 1/a]^4\}/ \\ & (\Gamma[p]\Gamma[1 - 2/a]\Gamma[p + 2/a] - \Gamma[1 - 1/a]^2\Gamma[p + 1/a]^2)^2.\end{aligned} \tag{A.9}$$

Thus, for given values of standard deviation (σ), skew (γ_3), and kurtosis (γ_4) associated with Dagum distribution, equations (A.7)-(A.9) can be used to simultaneously solve for the values of parameters p, a, and b. The solved values of p, a, and b can then be substituted into equation (A.6) to determine the value of mean.